

ADAPTIVITY AND BLOW-UP DETECTION FOR NONLINEAR EVOLUTION PROBLEMS

ANDREA CANGIANI*, EMMANUIL H. GEORGIOULIS*, IRENE KYZA†, AND STEPHEN
METCALFE*

Abstract. This work is concerned with the development of a space-time adaptive numerical method, based on a rigorous a posteriori error bound, for a semilinear convection-diffusion problem which may exhibit blow-up in finite time. More specifically, a posteriori error bounds are derived in the $L^\infty(L^2) + L^2(H^1)$ -type norm for a first order in time implicit-explicit (IMEX) interior penalty discontinuous Galerkin (dG) in space discretization of the problem, although the theory presented is directly applicable to the case of conforming finite element approximations in space. The choice of the discretization in time is made based on a careful analysis of adaptive time stepping methods for ODEs that exhibit finite time blow-up. The new adaptive algorithm is shown to accurately estimate the blow-up time of a number of problems, including one which exhibits regional blow-up.

Key words. finite time blow-up; conditional a posteriori error estimates; IMEX method; discontinuous Galerkin methods

1. Introduction. The numerical approximation of blow-up phenomena in partial differential equations (PDEs) is a challenging problem due to the high spatial and temporal resolution needed close to the blow-up time. Numerical methods giving good approximations close to the blow-up time include the rescaling algorithm of Berger and Kohn [8, 41] and the MMPDE method [9, 28]. There is also work looking at the numerical approximation of blow-up in the nonlinear Schrödinger equation and its generalizations [2, 12, 21, 32, 42, 45]. Other numerical methods for approximating blow-up can be found for a variety of different nonlinear PDEs [1, 3, 15, 18, 20, 25, 40] and ordinary differential equations (ODEs) [26, 29, 44]. Typically, these numerical methods rely on some form of theoretically justified rescaling but lack a rigorous justification as to whether the resulting numerical approximations are reasonable. In contrast, our approach is to perform numerical rescaling of a simple numerical scheme in an adaptive space-time setting driven by rigorous a posteriori error bounds.

A posteriori error estimators for finite element discretizations of nonlinear parabolic problems are available in the literature (e.g., [5, 6, 7, 11, 14, 24, 31, 46, 47, 48]). However, the literature on a posteriori error control for parabolic equations that exhibit finite time blow-up is very limited; to the best of our knowledge, only in [33] do the authors provide rigorous a posteriori error bounds for such problems. Using a semigroup approach, the authors of [33] arrive to *conditional* a posteriori error estimates in the $L^\infty(L^\infty)$ -norm for first and second order temporal semi-discretizations of a semilinear parabolic equation with polynomial nonlinearity. Conditional a posteriori error estimates have been derived in earlier works for several types of PDEs, see, e.g., [13, 22, 31, 35, 37]; the estimates are called conditional because they only hold under a computationally verifiable smallness condition.

In this work, we derive a practical conditional a posteriori bound for a fully-discrete first order in time implicit-explicit (IMEX) interior penalty discontinuous Galerkin (dG) in space discretization of a non self-adjoint semilinear parabolic PDE with quadratic nonlinearity. The choice of an IMEX discretization and, in particular,

*Department of Mathematics, University of Leicester, University Road, Leicester LE1 7RH, United Kingdom

†Department of Mathematics, University of Dundee, Nethergate, Dundee, DD1 4HN, United Kingdom

the explicit treatment of the nonlinearity, offers advantages in the context of finite time blow-up – this is highlighted below via the discretization of the related ODE problem with various time-stepping schemes. The choice of a dG method in space offers stability of the spatial operator in convection-dominated regimes on coarse meshes; we stress, however, that the theory presented below is directly applicable to the case of conforming finite element approximations in space. The conditional a posteriori error bounds are derived in the $L^\infty(L^2)+L^2(H^1)$ -type norm. The derivation is based on energy techniques combined with the Gagliardo-Nirenberg inequality while retaining the key idea introduced in [33] – judicious usage of Gronwall’s lemma. A key novelty of our approach is the use of a *local-in-time* continuation argument in conjunction with a space-time reconstruction. Global-in-time continuation arguments have been used to derive conditional a posteriori error estimates for finite element discretizations of PDEs with globally bounded solutions, cf. [5, 24, 31]. A useful by-product of the local continuation argument used in this work is that it gives a natural stopping criterion for approach towards the blow-up time. The use of space-time reconstruction, introduced in [34, 36] for conforming finite element methods and in [10, 23] for dG methods, allows for the derivation of a posteriori bounds in norms weaker than $L^2(H^1)$ and offers great flexibility in treating general spatial operators and their respective discretizations.

Furthermore, a space-time adaptive algorithm is proposed which uses the conditional a posteriori bound to control the time step lengths and the spatial mesh modifications. The adaptive algorithm is a non-trivial modification of typical adaptive error control procedures for parabolic problems. In the proposed adaptive algorithm, the tolerances are adapted in the run up to blow-up time to allow for larger absolute error in an effort to balance the relative error of the approximation. The space-time adaptive algorithm is tested on three numerical experiments, two of which exhibit point blow-up and one which exhibits regional blow-up. Each time the algorithm appears to detect and converge to the blow-up time without surpassing it.

The remainder of this work is structured as follows. In Section 2, we discuss the derivation of a posteriori bounds and algorithms for adaptivity for ODE problems whose solutions blow-up in finite time. Section 3 sets out the model problem and introduces some necessary notation while Section 4 discusses the discretization of the problem. Within Section 5 the proof of the conditional a posteriori error bound is presented. An adaptive algorithm based on this a posteriori bound is proposed in Section 6 followed by a series of numerical experiments in Section 7. Finally, some conclusions are drawn in Section 8.

2. Approximation of blow-up in ODEs. Before proceeding with the a posteriori error analysis and adaptivity of the semilinear PDE, it is illuminating to consider the numerical approximation of blow-up in the context of ODEs. To this end, we first analyse the ODE initial value problem: find $u : [0, T] \rightarrow \mathbb{R}$ such that

$$\begin{aligned} \frac{du}{dt} &= f(u) := \sum_{j=0}^p \alpha_j u^j, \quad \text{in } (0, T], \\ u(0) &= u_0, \end{aligned} \tag{2.1}$$

with $p \geq 2$ a positive integer and coefficients $\alpha_i \geq 0$, $i = 1, \dots, p-1$ and $\alpha_p > 0$ so that the solution blows up in finite time. Let T^* denote the blow-up time of (2.1) and assume $T < T^*$. For $t < T^*$, $u(t)$ is a differentiable function [27].

Let $0 \leq t^k \leq T$, $0 \leq k \leq N$ be defined by $t^k := t^{k-1} + \tau_k$ with $t^0 := 0$ and $t^N = T$ for some time step lengths $\tau_k > 0$, $k = 1, \dots, N$ with $\sum_{k=1}^N \tau_k = T$. We use the following three different one step schemes to approximate (2.1). We set $U^0 := u_0$ and, for $k = 1, \dots, N$, we seek U^k such that

$$\frac{U^k - U^{k-1}}{\tau_k} = F(U^{k-1}, U^k), \quad (2.2)$$

with F one of the following three classical approximations of f :

$$\begin{aligned} \text{Explicit Euler} \quad & F(U^{k-1}, U^k) = f(U^{k-1}), \\ \text{Implicit Euler} \quad & F(U^{k-1}, U^k) = f(U^k), \\ \text{Improved Euler} \quad & F(U^{k-1}, U^k) = 1/2 (f(U^{k-1}) + f(U^{k-1} + \tau_k f(U^{k-1}))). \end{aligned} \quad (2.3)$$

2.1. An a posteriori error estimate. We begin by defining $U : [0, T] \rightarrow \mathbb{R}$ by

$$U(t) := \ell_{k-1}(t)U^{k-1} + \ell_k(t)U^k, \quad t \in (t^{k-1}, t^k], \quad (2.4)$$

where $\{\ell_{k-1}, \ell_k\}$ denotes the standard linear Lagrange interpolation basis defined on the interval $[t^{k-1}, t^k]$, i.e., U is the continuous piecewise linear interpolant through the points (t^k, U^k) , $k = 0, \dots, N$. Hence, (2.2) can be equivalently written on each interval $(t^{k-1}, t^k]$ as

$$\frac{dU}{dt} = F(U^{k-1}, U^k). \quad (2.5)$$

Therefore, on each interval $(t^{k-1}, t^k]$, the error $e := u - U$ satisfies the equation

$$\frac{de}{dt} = f(u) - F(U^{k-1}, U^k) = f(U) + f'(U)e + \sum_{j=2}^p \frac{f^{(j)}(U)}{j!} e^j - F(U^{k-1}, U^k), \quad (2.6)$$

with $f^{(j)}$ denoting the order j derivative of f . Thus, upon defining the residual $\eta_k := f(U) - F(U^{k-1}, U^k)$, we obtain on each interval $(t^{k-1}, t^k]$ the primary error equation:

$$\frac{de}{dt} = \eta_k + f'(U)e + \sum_{j=2}^p \frac{f^{(j)}(U)}{j!} e^j. \quad (2.7)$$

Gronwall's inequality, therefore, implies that

$$|e(t)| \leq H_k(t)G_k\phi_k, \quad (2.8)$$

where

$$\begin{aligned} H_k(t) &:= \exp \left(\sum_{j=2}^p \int_{t^{k-1}}^t \frac{|f^{(j)}(U)|}{j!} |e|^{j-1} ds \right), \\ G_k &:= \exp \left(\int_{t^{k-1}}^{t^k} |f'(U)| ds \right), \\ \phi_k &:= |e(t^{k-1})| + \int_{t^{k-1}}^{t^k} |\eta_k| ds. \end{aligned} \quad (2.9)$$

From (2.8), we derive an a posteriori bound by a *local continuation argument*. To this end, we define the set

$$I_k := \left\{ t \in [t^{k-1}, t^k] : \max_{s \in [t^{k-1}, t]} |e(s)| \leq \delta_k G_k \phi_k \right\}, \quad (2.10)$$

for some $\delta_k > 1$ to be chosen below; note that $I_k \subset [t^{k-1}, t^k]$ and that I_k is closed since the error function e is continuous. The main idea is to use the continuity of the error function e and to choose δ_k implying that $I_k = [t^{k-1}, t^k]$ for each $k = 1, \dots, N$. Further, we will choose δ_k to be a computable bound of H_k thereby arriving to an a posteriori bound.

THEOREM 2.1 (Conditional a posteriori estimate). *Let u be the exact solution of (2.1), $\{U^k\}_{k=0}^N$ the approximations produced by (2.2) and U the piecewise linear interpolant (2.4). Then, for $k = 1, \dots, N$, the following a posteriori estimate holds:*

$$\max_{t \in [t^{k-1}, t^k]} |e(t)| \leq \delta_k G_k \phi_k, \quad (2.11)$$

provided that $\delta_k > 1$ is chosen so that

$$\sum_{j=2}^p (\delta_k G_k \phi_k)^{j-1} \int_{t^{k-1}}^{t^k} \frac{|f^{(j)}(U(s))|}{j!} ds - \log(\delta_k) = 0. \quad (2.12)$$

Proof. For $k = 1, \dots, N$, let I_k be as in (2.10) where $\delta_k > 1$ is chosen to satisfy

$$\exp \left(\sum_{j=2}^p (\delta_k G_k \phi_k)^{j-1} \int_{t^{k-1}}^{t^k} \frac{|f^{(j)}(U(s))|}{j!} ds \right) \leq (1 - \alpha) \delta_k, \quad (2.13)$$

for some $0 < \alpha < 1$. The interval I_k is closed and non-empty since $t^{k-1} \in I_k$; hence, it attains a maximum $t_*^k := \max I_k$. Suppose that $t_*^k < t^k$. In view of the definition of H_k , we have

$$H_k(t_*^k) \leq \exp \left(\sum_{j=2}^p (\delta_k G_k \phi_k)^{j-1} \int_{t^{k-1}}^{t_*^k} \frac{|f^{(j)}(U(s))|}{j!} ds \right) \leq (1 - \alpha) \delta_k < \delta_k, \quad (2.14)$$

as $t_*^k \in I_k$. Application of (2.14) to (2.8) yields

$$\max_{t \in [t^{k-1}, t_*^k]} |e(t)| < \delta_k G_k \phi_k. \quad (2.15)$$

This implies that t_*^k cannot be the maximal element of I_k – a contradiction. Hence, $t_*^k = t^k$ and, thus, $I_k = [t^{k-1}, t^k]$. Considering the case with equality in (2.13) and taking $\alpha \rightarrow 0$, we arrive at (2.12) and the proof is complete. \square

Choosing $\delta_k > 1$ satisfying (2.12) is equivalent to finding a root (ideally the smallest one) of

$$\sum_{j=2}^p \left((G_k \phi_k)^{j-1} \int_{t^{k-1}}^{t^k} \frac{f^{(j)}(U(s))}{j!} ds \right) x^{j-1} - \log(x),$$

in the interval $(1, +\infty)$. This is only possible if the coefficients of x^j , $j = 1, \dots, p-1$, are “sufficiently small”, i.e., only provided that the time steps length τ_k is small

enough. In this sense, (2.11) is a conditional a posteriori bound. In practice, condition (2.12) is implemented by applying Newton's method. If for some k the time step length τ_k is not small enough, Newton's method does not converge and the procedure terminates (cf. Algorithms 1 and 2 below). With the aid of the next lemma, we state a precise condition on the time step lengths τ_k which indeed ensures that (2.12) has a root $\delta_k > 1$.

LEMMA 2.2. *If $\sum_{j=1}^p jC_j e^j \leq 1$ then $s(x) = \sum_{j=1}^p C_j x^j - \log(x)$ with $C_j > 0$, $j = 1, \dots, p$, $p \in \mathbb{N}$ has a root in $(1, +\infty)$.*

Proof. We begin by noting that $s(x)$ is continuous in $[1, +\infty)$ and differentiable in $(1, +\infty)$ with $s(1) = \sum_{j=1}^p C_j > 0$ and $\lim_{x \rightarrow +\infty} s(x) = +\infty$. Therefore $s(x)$ has a root in $(1, +\infty)$ if and only if it attains a nonpositive minimum in this interval. Differentiating $s(x)$ gives $s'(x) = \sum_{j=1}^p jC_j x^{j-1} - x^{-1}$. Since the coefficients C_j satisfy $\sum_{j=1}^p jC_j e^j \leq 1$, we observe that

$$s'(e) = \sum_{j=1}^p jC_j e^{j-1} - e^{-1} \leq 0.$$

Also, $\lim_{x \rightarrow +\infty} s'(x) > 0$. Hence, there exists a critical point $x_* \in [e, +\infty)$ satisfying

$$\sum_{j=1}^p jC_j x_*^j = 1. \quad (2.16)$$

All that remains is to prove that $s(x_*) \leq 0$. Indeed, (2.16) leads to

$$\sum_{j=1}^p C_j x_*^j \leq \sum_{j=1}^p jC_j x_*^j = 1 \leq \log(x_*),$$

where the last inequality holds because $x_* \geq e$. From the above relation, we readily conclude that $s(x_*) \leq 0$ and the proof is complete. \square

The above lemma gives a sufficient condition on when (2.12) can be satisfied. In particular, condition (2.12) can always be made to be satisfied provided that the time step length τ_k is chosen such that

$$\sum_{j=2}^p \frac{j-1}{j!} (G_k \phi_k e)^{j-1} \int_{t^{k-1}}^{t^k} |f^{(j)}(U(s))| ds \leq 1.$$

Returning back to Theorem 2.1, we note that this gives a recursive procedure for the estimation of the error on each subinterval $[t^{k-1}, t^k]$. Indeed, the term $|e(t^{k-1})|$ in ϕ_k is estimated using the error estimator from the previous time step with $e(0) = 0$.

2.2. Adaptivity. Based upon the a posteriori error estimator presented in Theorem 2.1, we propose Algorithm 1 for advancing towards the blow-up time.

Assuming that the adaptive algorithm outputs successfully at time $T = T(\text{tol}, N)$ for a given tolerance tol and after total number of time steps N then we are interested in observing the order of convergence as $T \rightarrow T^*$ with respect to N . To this end, we define the function $\lambda(\text{tol}, N) := |T^* - T(\text{tol}, N)|$ where T^* is the blow-up time of (2.1) and we numerically investigate the rate $r > 0$ such that

$$\lambda(\text{tol}, N) \propto N^{-r}. \quad (2.17)$$

Algorithm 1 ODE Algorithm 1

```

1: Input:  $f, F, u_0, \tau_1, \mathbf{tol}$ .
2: Compute  $U^1$  from  $U^0$ .
3: while  $\int_{t^0}^{t^1} |\eta_1| ds > \mathbf{tol}$  do
4:    $\tau_1 \leftarrow \tau_1/2$ .
5:   Compute  $U^1$  from  $U^0$ .
6: end while
7: Compute  $\delta_1$ .
8: Set  $k = 0$ .
9: while  $\delta_{k+1}$  exists do
10:   $k \leftarrow k + 1$ .
11:   $\tau_{k+1} = \tau_k$ .
12:  Compute  $U^{k+1}$  from  $U^k$ .
13:  while  $\int_{t^k}^{t^{k+1}} |\eta_{k+1}| ds > \mathbf{tol}$  do
14:     $\tau_{k+1} \leftarrow \tau_{k+1}/2$ .
15:    Compute  $U^{k+1}$  from  $U^k$ .
16:  end while
17:  Compute  $\delta_{k+1}$ .
18: end while
19: Output:  $k, t^k$ .

```

One may initially expect that r would be equal to the order of the time-stepping scheme used. To gain insight into the rate convergence of λ , we apply Algorithm 1 to (2.1) with $f(u) = u^p$ for $p = 2, 3$ and $u(0) = 1$ for each of the three time-stepping schemes (2.3). The computed rates of convergence r under Algorithm 1 are given in Table 2.1.

Table 2.1: Algorithm 1 Results

Method	$p = 2$	$p = 3$
Implicit Euler	$r \approx 0.66$	$r \approx 0.79$
Explicit Euler	$r \approx 1.35$	$r \approx 1.60$
Improved Euler	$r \approx 1.2$	$r \approx 1.48$

Somewhat surprisingly at first sight, the explicit Euler scheme performs significantly better than the implicit Euler scheme. This fact can be explained by looking back at the derivation of the error estimator. The explicit Euler scheme always underestimates the true solution u [44].

This, in turn, implies that δ_{k+1} is correcting for the fact that G_{k+1} is underestimating the true blow-up rate resulting in a tight a posteriori error bound and, thus, explaining the high rate of convergence of λ . When using the implicit Euler method, on the other hand, G_{k+1} overestimates the true blow-up rate [44] thereby conferring no additional benefit.

Note also that for both the implicit and improved Euler methods, the rate of convergence r is less than their formal orders of convergence, i.e., first and second

order, respectively. Moreover, one would expect a faster approach to the blow-up time using the second order improved Euler compared to the first order explicit Euler scheme. This unexpected behaviour is due to the way the tolerance is utilized in Algorithm 1. Indeed, Algorithm 1 aims to reduce the error under an absolute tolerance tol ; this is the standard practice in adaptive algorithms applied to linear problems. In the context of blow-up problems, however, the presence of the growth factor G_{k+1} cannot be neglected; requiring the adaptivity to be driven by an absolute tolerance in the run up to the blow up time results in excessive over-refinement and, thus, loss of the expected rate of convergence. To address this issue, we propose Algorithm 2 which increases tol proportionally to G_{k+1} allowing for control of the relative error (cf. line 19 in Algorithm 2).

Algorithm 2 ODE Algorithm 2

```

1: Input:  $f, F, u_0, \tau_1, \text{tol}$ .
2: Compute  $U^1$  from  $U^0$ .
3: while  $\int_{t^0}^{t^1} |\eta_1| ds > \text{tol}$  do
4:    $\tau_1 \leftarrow \tau_1/2$ .
5:   Compute  $U^1$  from  $U^0$ .
6: end while
7: Compute  $\delta_1$ .
8:  $\text{tol} = G_1 * \text{tol}$ .
9: Set  $k = 0$ .
10: while  $\delta_{k+1}$  exists do
11:    $k \leftarrow k + 1$ .
12:    $\tau_{k+1} = \tau_k$ .
13:   Compute  $U^{k+1}$  from  $U^k$ .
14:   while  $\int_{t^k}^{t^{k+1}} |\eta_{k+1}| ds > \text{tol}$  do
15:      $\tau_{k+1} \leftarrow \tau_{k+1}/2$ .
16:     Compute  $U^{k+1}$  from  $U^k$ .
17:   end while
18:   Compute  $\delta_{k+1}$ .
19:    $\text{tol} = G_{k+1} * \text{tol}$ .
20: end while
21: Output:  $k, t^k$ .

```

Table 2.2: Algorithm 2 Results

Method	$p = 2$	$p = 3$
Implicit Euler	$r \approx 1.00$	$r \approx 1.00$
Explicit Euler	$r \approx 1.45$	$r \approx 1.43$
Improved Euler	$r \approx 2.03$	$r \approx 2.03$

The rates of convergence r of λ under Algorithm 2 are given in Table 2.2. The theoretically conjectured orders of convergence for both the implicit and improved Euler schemes are recovered while the explicit Euler method still outperforms its

expected rate. In the case $p = 3$ (cubic nonlinearity) and for the explicit Euler method only, Algorithm 1 converges somewhat faster than Algorithm 2. The reason for this behaviour is unclear and requires further investigation.

3. Model problem. Let $\Omega \subset \mathbb{R}^2$ be the computational domain which is assumed to be a bounded polygon with Lipschitz boundary $\partial\Omega$. We denote the standard L^2 -inner product on $\omega \subseteq \Omega$ by $(\cdot, \cdot)_\omega$ and the standard L^2 -norm by $\|\cdot\|_\omega$; when $\omega = \Omega$ these will be abbreviated to (\cdot, \cdot) and $\|\cdot\|$, respectively. We shall also make use of the standard Sobolev spaces $W^{k,p}(\omega)$ along with the standard notation $L^p(\omega) = W^{0,p}(\omega)$, $1 \leq p \leq \infty$; $H^k(\omega) := W^{k,2}(\omega)$, $k \geq 0$; and $H_0^1(\Omega)$ denoting the subspace of $H^1(\Omega)$ consisting of functions vanishing on the boundary $\partial\Omega$. For $T > 0$ and a real Banach space X with norm $\|\cdot\|_X$, we define the spaces $L^p(0, T; X)$ consisting of all measurable functions $v : [0, T] \rightarrow X$ for which

$$\begin{aligned} \|v\|_{L^p(0,T;X)} &:= \left(\int_0^T \|v(t)\|_X^p dt \right)^{1/p} < \infty, & \text{for } 1 \leq p < +\infty, \\ \|v\|_{L^p(0,T;X)} &:= \operatorname{ess\,sup}_{0 \leq t \leq T} \|v(t)\|_X < \infty, & \text{for } p = +\infty. \end{aligned}$$

We also define $H^1(0, T, X) := \{u \in L^2(0, T; X) : u_t \in L^2(0, T; X)\}$ and we denote by $C(0, T; X)$ the space of continuous functions $v : [0, T] \rightarrow X$ such that

$$\|v\|_{C(0,T;X)} := \max_{0 \leq t \leq T} \|v(t)\|_X < \infty.$$

The model problem consists of finding $u : \Omega \times (0, T] \rightarrow \mathbb{R}$ such that

$$\begin{aligned} \frac{\partial u}{\partial t} - \varepsilon \Delta u + \mathbf{a} \cdot \nabla u + f(u) &= 0 & \text{in } \Omega \times (0, T], \\ u &= 0 & \text{on } \partial\Omega \times (0, T], \\ u(\cdot, 0) &= u_0 & \text{in } \bar{\Omega}, \end{aligned} \tag{3.1}$$

for $f(u) = f_0 - u^2$ and where $u_0 \in H_0^1(\Omega)$, $\varepsilon > 0$, $\mathbf{a} \in [C(0, T; W^{1,\infty}(\Omega))]^2$ and $f_0 \in C(0, T; L^2(\Omega))$. For simplicity of the presentation only, we shall also assume that $\nabla \cdot \mathbf{a} = 0$ although this is not an essential restriction to the analysis that follows.

The weak form of (3.1) reads: find $u \in L^2(0, T; H_0^1(\Omega)) \cap H^1(0, T; L^2(\Omega))$ such that for almost every $t \in (0, T]$ we have

$$\left(\frac{\partial u}{\partial t}, v \right) + B(t; u, v) + (f(t; u), v) = 0 \quad \forall v \in H_0^1(\Omega), \tag{3.2}$$

where

$$B(t; u, v) := \int_\Omega (\varepsilon \nabla u - \mathbf{a}u) \cdot \nabla v dx.$$

Under the above assumptions and for any $t \in (0, T]$ the bilinear form B is coercive in and $H_0^1(\Omega)$, viz., $B(t; v, v) \geq \varepsilon \|\nabla v\|^2$, for all $v \in H_0^1(\Omega)$.

4. Discretization. Consider a shape-regular mesh $\zeta = \{K\}$ of Ω with K denoting a generic element that is constructed via affine mappings $F_K : \hat{K} \rightarrow K$ with non-singular Jacobian where \hat{K} is the reference triangle or the reference square. The

mesh is allowed to contain a uniformly fixed number of regular hanging nodes per edge. On ζ , we define the finite element space

$$\mathbb{V}_h(\zeta) := \{v \in L^2(\Omega) : v|_K \circ F_K \in \mathcal{P}^p(\hat{K}), K \in \zeta\}, \quad (4.1)$$

with $\mathcal{P}^p(K)$ denoting the space of polynomials of total degree p or of degree p in each variable if \hat{K} is the reference triangle or the reference square, respectively. In what follows, we shall often make use of the orthogonal L^2 -projection onto the finite element space \mathbb{V}_h^k , which we will denote by Π^k .

The set of all edges in the triangulation ζ is denoted by $\mathcal{E}(\zeta)$ while $\mathcal{E}^{int}(\zeta) \subset \mathcal{E}(\zeta)$ stands for the subset of all interior edges. Given $K \in \zeta$ and $E \in \mathcal{E}(\zeta)$, we set $h_K := \text{diam}(K)$ and $h_E := \text{diam}(E)$, respectively; we also denote the outward unit normal to the boundary ∂K by \mathbf{n}_K . Given an edge $E \in \mathcal{E}^{int}(\zeta)$ shared by two elements K and K' , a vector field $\mathbf{v} \in [H^{1/2}(\Omega)]^2$ and a scalar field $v \in H^{1/2}(\Omega)$, we define jumps and averages of \mathbf{v} and v across E by

$$\begin{aligned} \{\mathbf{v}\} &:= \frac{1}{2}(\mathbf{v}|_{E \cap \bar{K}} + \mathbf{v}|_{E \cap \bar{K}'}), & [\mathbf{v}] &:= \mathbf{v}|_{E \cap \bar{K}} \cdot \mathbf{n}_K + \mathbf{v}|_{E \cap \bar{K}'} \cdot \mathbf{n}_{K'}, \\ \{v\} &:= \frac{1}{2}(v|_{E \cap \bar{K}} + v|_{E \cap \bar{K}'}), & [v] &:= v|_{E \cap \bar{K}} \mathbf{n}_K + v|_{E \cap \bar{K}'} \mathbf{n}_{K'}. \end{aligned}$$

If $E \subset \partial\Omega$, we set $\{\mathbf{v}\} := \mathbf{v}$, $[\mathbf{v}] := \mathbf{v} \cdot \mathbf{n}$, $\{v\} := v$ and $[v] := v\mathbf{n}$ with \mathbf{n} denoting the outward unit normal to the boundary $\partial\Omega$. The inflow and outflow parts of the boundary $\partial\Omega$ at time t , respectively, are defined by

$$\partial\Omega_{in}^t := \{x \in \partial\Omega : \mathbf{a}(x, t) \cdot \mathbf{n}(x) < 0\}, \quad \partial\Omega_{out}^t := \{x \in \partial\Omega : \mathbf{a}(x, t) \cdot \mathbf{n}(x) \geq 0\}.$$

Similarly, the inflow and outflow parts of an element K at time t are defined by

$$\partial K_{in}^t := \{x \in \partial K : \mathbf{a}(x, t) \cdot \mathbf{n}_K(x) < 0\}, \quad \partial K_{out}^t := \{x \in \partial K : \mathbf{a}(x, t) \cdot \mathbf{n}_K(x) \geq 0\}.$$

We consider an implicit-explicit (IMEX) space-time discretization of (3.2) consisting of implicit treatment for the linear convection-diffusion terms and explicit treatment for the nonlinear reaction term which was shown to be beneficial in Section 2. For the spatial discretization, we use a standard (upwinded) interior penalty discontinuous Galerkin method, detailed below, to ensure stability of the spatial operator in convection-dominated regimes.

To this end, we consider a subdivision of $[0, T]$ into time intervals of lengths τ_1, \dots, τ_N such that $\sum_{j=1}^N \tau_j = T$ for some integer $N \geq 1$ and we set $t^0 := 0$ and $t^k := \sum_{j=1}^k \tau_j$, $k = 1, \dots, N$. Let ζ^0 denote an initial spatial mesh of Ω associated with the time $t^0 = 0$. To each time t^k , $k = 1, \dots, N$, we associate the spatial mesh ζ^k of Ω which is assumed to have been obtained from ζ^{k-1} by local refinement and/or coarsening. Each mesh ζ^k is assigned the finite element space $\mathbb{V}_h^k := \mathbb{V}_h(\zeta^k)$ given by (4.1). For brevity, let $\mathbf{a}^k := \mathbf{a}(\cdot, t^k)$ and $f^k := f(\cdot, t^k; U_h^k)$. Finally, for $t \in (t^{k-1}, t^k]$, $\Gamma(t)$ will denote the union of all edges in the coarsest common refinement $\zeta^{k-1} \cup \zeta^k$ of ζ^{k-1} and ζ^k .

The IMEX dG method then reads as follows. Let U_h^0 be a projection of u_0 onto \mathbb{V}_h^0 . For $k = 1, \dots, n$, find $U_h^k \in \mathbb{V}_h^k$ such that

$$\left(\frac{U_h^k - U_h^{k-1}}{\tau_k}, v_h^k \right) + B(t^k; U_h^k, v_h^k) + K_h(U_h^k, v_h^k) + (f^{k-1}, v_h^k) = 0, \quad (4.2)$$

for all $v_h^k \in \mathbb{V}_h^k$ where

$$\begin{aligned} B(t^k; U_h^k, v_h^k) &:= \sum_{K \in \zeta^k} \int_K (\varepsilon \nabla U_h^k - \mathbf{a} U_h^k) \cdot \nabla v_h^k \, dx + \sum_{E \in \mathcal{E}(\zeta^k)} \frac{\gamma \varepsilon}{h_E} \int_E [U_h^k] \cdot [v_h^k] \, ds \\ &\quad + \sum_{K \in \zeta^k} \int_{\partial K_{out}^{t^k}} U_h^k [\mathbf{a} v_h^k] \, ds, \\ K_h(U_h^k, v_h^k) &:= - \sum_{E \in \mathcal{E}(\zeta^k)} \int_E \{\varepsilon \nabla U_h^k\} \cdot [v_h^k] + \{\varepsilon \nabla v_h^k\} \cdot [U_h^k] \, ds. \end{aligned}$$

We shall choose U_h^0 as the orthogonal L^2 -projection of u_0 onto \mathbb{V}_h^0 , that is $U_h^0 := \Pi^0 u_0$, although other projections onto \mathbb{V}_h^0 can also be used. In standard fashion, the penalty parameter, γ , is chosen large enough so that the operator $B + K_h$ is coercive on \mathbb{V}_h^k (see, e.g., [17]).

5. An a posteriori bound. In the context of the elliptic reconstruction framework [34, 36], we require an a posteriori error bound for a related stationary problem. To that end, we consider a generalization of the error bound introduced in [43]; the proof of such bound is completely analogous and is, therefore, omitted for brevity.

THEOREM 5.1. *Given $t \in (0, T]$ and $g \in L^2(\Omega)$, let $u^s \in H_0^1(\Omega)$ be the exact solution of the elliptic problem*

$$B(t; u^s, v) = (g, v),$$

for all $v \in H_0^1(\Omega)$ and let $u_h^s \in \mathbb{V}_h$ such that

$$B(t; u_h^s, v_h) + K_h(u_h^s, v_h) = (g, v_h),$$

for all $v_h \in \mathbb{V}_h$ be its dG approximation. Then the following a posteriori error bound holds for any $0 \neq v \in H_0^1(\Omega)$:

$$\begin{aligned} \left(\frac{B(u^s - u_h^s, v)}{\sqrt{\varepsilon} \|\nabla v\|} \right)^2 &\lesssim \sum_{K \in \zeta} \frac{h_K^2}{\varepsilon} \|g + \varepsilon \Delta u_h^s - \mathbf{a} \cdot \nabla u_h^s\|_K^2 + \sum_{E \in \mathcal{E}^{int}(\zeta)} \varepsilon h_E \|\nabla u_h^s\|_E^2 \\ &\quad + \sum_{E \in \mathcal{E}(\zeta)} \frac{\gamma \varepsilon}{h_E} \|[u_h^s]\|_E^2 + \frac{h_E}{\varepsilon} \|\mathbf{a} u_h^s\|_E^2. \end{aligned}$$

The symbols \lesssim and \gtrsim used above and throughout the rest of this section denote inequalities true up to a constant independent of the data ε , \mathbf{a} , f , the exact and numerical solutions u , u_h , and the local mesh-sizes and time step lengths.

DEFINITION 5.2. *We denote by $A^k \in \mathbb{V}_h^k$ the unique solution of the problem*

$$B(t^k; U_h^k, v_h^k) + K_h(U_h^k, v_h^k) = (A^k, v_h^k) \quad \forall v_h^k \in \mathbb{V}_h^k.$$

For $k \geq 1$, we observe that $A^k = -\Pi^k f^{k-1} - (U_h^k - \Pi^k U_h^{k-1})/\tau_k$ from (4.2).

DEFINITION 5.3. *We define the elliptic reconstruction $w^k \in H_0^1(\Omega)$, $k = 0, \dots, N$, to be the unique solution of the elliptic problem*

$$B(t^k; w^k, v) = (A^k, v) \quad \forall v \in H_0^1(\Omega).$$

Crucially, the dG discretization of the elliptic problem in Definition 5.3 is equal to U_h^k and so $B(t^k; w^k - U_h^k, v)$ can be estimated by Theorem 5.1.

At each time step k , we decompose the dG solution U_h^k into a conforming part $U_{h,c}^k \in H_0^1(\Omega) \cap \mathbb{V}_h^k$ and a non-conforming part $U_{h,d}^k \in \mathbb{V}_h^k$ such that $U_h^k = U_{h,c}^k + U_{h,d}^k$.

Further, for $t \in (t^{k-1}, t^k]$, we define $U_h(t)$ to be the linear interpolant with respect to t of the values U_h^{k-1} and U_h^k , viz.,

$$U_h(t) := \ell_{k-1}(t)U_h^{k-1} + \ell_k(t)U_h^k,$$

where, as before, $\{\ell_{k-1}, \ell_k\}$ denotes the standard linear Lagrange interpolation basis defined on the interval $[t^{k-1}, t^k]$. We define $U_{h,c}(t)$ and $U_{h,d}(t)$ analogously. We then decompose the error $e := u - U_h = e_c - U_{h,d}$ with $e_c := u - U_{h,c}$ and we denote the elliptic error by $\theta^k := w^k - U_h^k$.

THEOREM 5.4. *Given $t \in [t^{k-1}, t^k]$, there exists a decomposition of U_h , as described above, such that the following bounds hold for each element $K \in \zeta^{k-1} \cup \zeta^k$:*

$$\begin{aligned} \|\nabla U_{h,d}\|_K^2 &\lesssim \sum_{E \subset \bar{K}_E} h_E^{-1} \| [U_h] \|_E^2, \\ \|U_{h,d}\|_K^2 &\lesssim \sum_{E \subset \bar{K}_E} h_E \| [U_h] \|_E^2, \\ \|U_{h,d}\|_{L^\infty(K)} &\lesssim \| [U_h] \|_{L^\infty(\bar{K}_E)}, \end{aligned}$$

where $\bar{K}_E := \{\cup E : \bar{K} \cap \bar{E} \neq \emptyset, E \in \mathcal{E}(\zeta^k \cup \zeta^{k+1})\}$ denotes the edge patch of the element K – the union of all edges with a vertex on ∂K .

Proof. See [30] for the first two estimates and [16] for the final estimate. \square

LEMMA 5.5. *Let $t \in (t^{k-1}, t^k]$ then for any $v \in H_0^1(\Omega)$ we have*

$$\left(\frac{\partial e}{\partial t}, v \right) + B(t; e, v) + (f(t; u) - f(t; U_h), v) = \left(-f(t; U_h) - \frac{\partial U_h}{\partial t}, v \right) - B(t; U_h, v).$$

Proof. This follows from (3.2). \square

From Lemma 5.5 we obtain

$$\begin{aligned} \left(\frac{\partial e}{\partial t}, v \right) + B(t; e, v) + (f(t; u) - f(t; U_h), v) &= - \left(A^k + f^{k-1} + \frac{\partial U_h}{\partial t}, v \right) \\ &+ B(t^k; \theta^k, v) - B(t; U_h, v) + B(t^k; U_h^k, v) + (f^{k-1} - f(t; U_h), v), \end{aligned} \quad (5.1)$$

which, upon straightforward manipulation, gives

$$\begin{aligned} \left(\frac{\partial e}{\partial t}, v \right) + B(t; e, v) + (f(t; u) - f(t; U_h), v) &= - \left(A^k + f^{k-1} + \frac{\partial U_h}{\partial t}, v \right) \\ &+ \ell_{k-1} B(t^{k-1}; \theta^{k-1}, v) + \ell_k B(t^k; \theta^k, v) - B(t; U_h, v) + \ell_{k-1} B(t^{k-1}; U_h^{k-1}, v) \\ &+ \ell_k B(t^k; U_h^k, v) + (f^{k-1} - f(t; U_h) + \ell_{k-1}(A^k - A^{k-1}), v). \end{aligned} \quad (5.2)$$

In what follows, it will be convenient to define the a posteriori error estimator through three constituent terms η_I , η_A , and η_B . The first part of the estimator is the initial condition estimator, η_I , given by

$$\eta_I := \left(\|e(0)\|^2 + \sum_{E \in \mathcal{E}(\zeta^0)} h_E \| [U_h^0] \|_E^2 \right)^{1/2}.$$

Both remaining parts, η_A and η_B , are the sum of a number of terms related to either a space or time discretisation error, identified by a subscript S or T , respectively. In this way, for $t \in (t^{k-1}, t^k]$, η_A is given by

$$\eta_A := \ell_{k-1} \eta_{S_1, k-1} + \ell_k \eta_{S_1, k} + \eta_{S_2, k} + \eta_{T_1, k},$$

where

$$\begin{aligned}\eta_{S_1,k} &:= \left(\sum_{K \in \zeta^k} \frac{h_K^2}{\varepsilon} \|A^k + \varepsilon \Delta U_h^k - \mathbf{a}^k \cdot \nabla U_h^k\|_K^2 + \sum_{E \in \mathcal{E}^{int}(\zeta^k)} \varepsilon h_E \|\nabla U_h^k\|_E^2 \right. \\ &\quad \left. + \sum_{E \in \mathcal{E}(\zeta^k)} \frac{\gamma \varepsilon}{h_E} \|[U_h^k]\|_E^2 + \frac{h_E}{\varepsilon} \|[\mathbf{a}^k U_h^k]\|_E^2 \right)^{1/2}, \\ \eta_{S_2,k} &:= \left(\sum_{K \in \zeta^{k-1} \cup \zeta^k} \frac{h_K^2}{\varepsilon} \|f^{k-1} - \Pi^k f^{k-1} - (U_h^{k-1} - \Pi^k U_h^{k-1})/\tau_k\|_K^2 \right)^{1/2}, \\ \eta_{T_1,k} &:= \varepsilon^{-1/2} \|\ell_{k-1}(\mathbf{a}^{k-1} - \mathbf{a})U_h^{k-1} + \ell_k(\mathbf{a}^k - \mathbf{a})U_h^k\|,\end{aligned}$$

while η_B is given by

$$\eta_B := \eta_{S_3,k} + \eta_{S_4,k} + \eta_{T_2,k},$$

where

$$\begin{aligned}\eta_{S_3,k} &:= \left(\sum_{K \in \zeta^{k-1} \cup \zeta^k} \sum_{E \subset \bar{K}_E} \sigma_K^2 h_E \|[U_h]\|_E^2 \right)^{1/2}, \\ \eta_{S_4,k} &:= \left(\sum_{E \subset \Gamma(t)} h_E \|[U_h^k - U_h^{k-1}]/\tau_k\|_E^2 \right)^{1/2}, \\ \eta_{T_2,k} &:= \|f^{k-1} - f(t; U_h) + \ell_{k-1}(A^k - A^{k-1})\|,\end{aligned}$$

with

$$\sigma_K := 2\|U_h\|_{L^\infty(K)} + \|[U_h]\|_{L^\infty(\bar{K}_E)}.$$

With the above notation at hand, we go back to (5.2) and bound the first term on the right-hand side using the definition of A^k , the orthogonality property of the L^2 -projection and the Cauchy-Schwarz inequality:

$$\begin{aligned}\left(A^k + f^{k-1} + \frac{\partial U_h}{\partial t}, v \right) &= \left(f^{k-1} - \Pi^k f^{k-1} - \frac{U_h^{k-1} - \Pi^k U_h^{k-1}}{\tau_k}, v - \Pi^k v \right) \\ &\lesssim \eta_{S_2,k} \sqrt{\varepsilon} \|\nabla v\|.\end{aligned}\quad (5.3)$$

The next two terms give rise to parts of the space estimator via Theorem 5.1:

$$\ell_{k-1} B(t^{k-1}; \theta^{k-1}, v) + \ell_k B(t^k; \theta^k, v) \lesssim (\ell_{k-1} \eta_{S_1,k-1} + \ell_k \eta_{S_1,k}) \sqrt{\varepsilon} \|\nabla v\|. \quad (5.4)$$

Using the definition of the bilinear form B and the Cauchy-Schwarz inequality, the final four terms give rise to the time estimator:

$$\begin{aligned}\ell_{k-1} B(t^{k-1}; U_h^{k-1}, v) + \ell_k B(t^k; U_h^k, v) - B(t; U_h, v) &\leq \eta_{T_1,k} \sqrt{\varepsilon} \|\nabla v\|, \\ (f^{k-1} - f(t; U_h) + \ell_{k-1}(A^k - A^{k-1}), v) &\leq \eta_{T_2,k} \|v\|.\end{aligned}\quad (5.5)$$

Setting $v = e_c$ in (5.2), using the results above along with the coercivity of the bilinear form B and the Cauchy-Schwarz inequality, we obtain

$$\begin{aligned}\frac{1}{2} \frac{d}{dt} \|e_c\|^2 + \varepsilon \|\nabla e_c\|^2 + (f(t; u) - f(t; U_h), e_c) &\lesssim \left(\left\| \frac{\partial U_{h,d}}{\partial t} \right\| + \eta_{T_2,k} \right) \|e_c\| \\ &+ (\ell_{k-1} \eta_{S_1,k-1} + \ell_k \eta_{S_1,k} + \eta_{S_2,k} + \eta_{T_1,k}) \sqrt{\varepsilon} \|\nabla e_c\| + B(t; U_{h,d}, e_c).\end{aligned}\quad (5.6)$$

Application of Theorem 5.4 implies that

$$\begin{aligned} \frac{1}{2} \frac{d}{dt} \|e_c\|^2 + \varepsilon \|\nabla e_c\|^2 + (f(t; u) - f(t; U_h), e_c) &\lesssim (\eta_{S_4, k} + \eta_{T_2, k}) \|e_c\| \\ &+ (\ell_{k-1} \eta_{S_1, k-1} + \ell_k \eta_{S_1, k} + \eta_{S_2, k} + \eta_{T_1, k}) \sqrt{\varepsilon} \|\nabla e_c\|. \end{aligned} \quad (5.7)$$

Thus, we conclude that

$$\frac{1}{2} \frac{d}{dt} \|e_c\|^2 + \frac{\varepsilon}{2} \|\nabla e_c\|^2 + (f(t; u) - f(t; U_h), e_c) \lesssim \frac{1}{2} \eta_A^2 + \eta_B \|e_c\|. \quad (5.8)$$

We must now deal with the nonlinear term on the left-hand side of (5.8). We begin by noting that

$$(f(t; u) - f(t; U_h), e_c) = (f(t; e_c - U_{h,d} + U_h) - f(t; U_h), e_c) = T_1 + T_2, \quad (5.9)$$

where

$$\begin{aligned} T_1 &:= (2U_h U_{h,d}, e_c) - (U_{h,d}^2, e_c), \\ T_2 &:= -(2U_h e_c, e_c) + (2e_c U_{h,d}, e_c) - (e_c^2, e_c). \end{aligned}$$

Upon writing the contributions to T_1 elementwise and using Theorem 5.4, we have

$$\begin{aligned} |T_1| &\leq \left(\sum_{K \in \zeta^{k-1} \cup \zeta^k} (2\|U_h\|_{L^\infty(K)} + \|U_{h,d}\|_{L^\infty(K)})^2 \|U_{h,d}\|_K^2 \right)^{1/2} \|e_c\| \\ &\lesssim \eta_{S_3, k} \|e_c\|. \end{aligned} \quad (5.10)$$

To bound T_2 , we use Hölder's inequality along with Theorem 5.4 to conclude that

$$|T_2| \lesssim (2\|U_h\|_{L^\infty(\Omega)} + \|[U_h]\|_{L^\infty(\Gamma(t))}) \|e_c\|^2 + \|e_c\|_{L^3(\Omega)}^3. \quad (5.11)$$

Combining (5.8), (5.9), (5.10) and (5.11) we obtain

$$\frac{d}{dt} \|e_c\|^2 + \varepsilon \|\nabla e_c\|^2 \leq C\eta_A^2 + 2C\eta_B \|e_c\| + 2\sigma_\Omega \|e_c\|^2 + 2\|e_c\|_{L^3(\Omega)}^3, \quad (5.12)$$

with $\sigma_\Omega := 2\|U_h\|_{L^\infty(\Omega)} + C\|[U_h]\|_{L^\infty(\Gamma(t))}$ where $C > 0$ is a constant that is independent of ε , \mathbf{a} , f , u , U_h and the local mesh-sizes and time step lengths. For $v \in H_0^1(\Omega)$, the Gagliardo-Nirenberg inequality $\|v\|_{L^3(\Omega)}^3 \leq C_{\text{GN}} \|v\|^2 \|\nabla v\|$ implies that

$$\|e_c\|_{L^3(\Omega)}^3 \leq C_{\text{GN}} \|e_c\|^2 \|\nabla e_c\| \leq \frac{\varepsilon}{2} \|\nabla e_c\|^2 + \frac{C_{\text{GN}}^2}{2\varepsilon} \|e_c\|^4. \quad (5.13)$$

Thus,

$$\frac{d}{dt} \|e_c\|^2 \leq C\eta_A^2 + 2C\eta_B \|e_c\| + 2\sigma_\Omega \|e_c\|^2 + C_{\text{GN}}^2 \varepsilon^{-1} \|e_c\|^4. \quad (5.14)$$

To deal with the L^2 -norms of e_c appearing on the right-hand side, we use a variant of Gronwall's inequality.

THEOREM 5.6. *Let $T > 0$ and suppose that c_0 is a constant, $c_1, c_2 \in L^1(0, T)$ are non-negative functions and that $u \in W^{1,1}(0, T)$ is a non-negative function satisfying*

$$u^2(T) \leq c_0^2 + \int_0^T c_1(s) u(s) \, ds + \int_0^T c_2(s) u^2(s) \, ds,$$

then

$$u(T) \leq \left(|c_0| + \frac{1}{2} \int_0^T c_1(s) ds \right) \exp \left(\frac{1}{2} \int_0^T c_2(s) ds \right).$$

Proof. See Theorem 21 in [19]. \square

Application of Theorem 5.6 to (5.14) for $t \in (t^{k-1}, t^k]$ yields

$$\|e_c(t)\| \leq \mathcal{H}_k(t) \mathcal{G}_k \Phi_k, \quad (5.15)$$

where

$$\begin{aligned} \Phi_k &:= \left(\|e_c(t^{k-1})\|^2 + C \int_{t^{k-1}}^{t^k} \eta_A^2 ds \right)^{1/2} + C \int_{t^{k-1}}^{t^k} \eta_B ds, \\ \mathcal{G}_k &:= \exp \left(\int_{t^{k-1}}^{t^k} \sigma_\Omega ds \right), \\ \mathcal{H}_k(t) &:= \exp \left(C_{GN}^2 \varepsilon^{-1} \int_{t^{k-1}}^t \|e_c\|^2 ds \right). \end{aligned}$$

To remove the non-computable term \mathcal{H}_k from (5.15), we use a continuation argument. We define the set

$$\mathcal{I}_k := \{t \in [t^{k-1}, t^k] : \|e_c\|_{L^\infty(t^{k-1}, t; L^2(\Omega))} \leq \delta_k \mathcal{G}_k \Phi_k\},$$

where, analogous to the ODE case, $\delta_k > 1$ should be chosen as small as possible. \mathcal{I}_k is non-empty (since $t^{k-1} \in \mathcal{I}_k$) and bounded and, thus, attains some maximum value. Let $t^* = \max \mathcal{I}_k$ and assume that $t^* < t^k$. Then, from (5.15), we have

$$\begin{aligned} \|e_c\|_{L^\infty(t^{k-1}, t^*; L^2(\Omega))} &\leq \mathcal{H}(t^*) \mathcal{G}_k \Phi_k \\ &\leq \exp(C_{GN}^2 \varepsilon^{-1} \tau_k \|e_c\|_{L^\infty(t^{k-1}, t^*; L^2(\Omega))}^2) \mathcal{G}_k \Phi_k \\ &\leq \exp(C_{GN}^2 \varepsilon^{-1} \tau_k \delta_k^2 \mathcal{G}_k^2 \Phi_k^2) \mathcal{G}_k \Phi_k. \end{aligned} \quad (5.16)$$

Now, suppose $\delta_k > 1$ is chosen such that

$$\exp(C_{GN}^2 \varepsilon^{-1} \tau_k \delta_k^2 \mathcal{G}_k^2 \Phi_k^2) \leq (1 - \alpha) \delta_k, \quad (5.17)$$

for some $0 < \alpha < 1$ then (5.16) gives

$$\|e_c\|_{L^\infty(t^{k-1}, t^*; L^2(\Omega))} \leq (1 - \alpha) \delta_k \mathcal{G}_k \Phi_k < \delta_k \mathcal{G}_k \Phi_k, \quad (5.18)$$

which, in turn, implies that t^* cannot be the maximal value of t in \mathcal{I}_k – a contradiction. Hence $\mathcal{I}_k = [t^{k-1}, t^k]$ and we have the desired error bound once δ_k is selected. Taking $\alpha \rightarrow 0$, we can select $\delta_k > 1$ to be the smallest root of

$$C_{GN}^2 \varepsilon^{-1} \tau_k \delta_k^2 \mathcal{G}_k^2 \Phi_k^2 - \log(\delta_k) = 0. \quad (5.19)$$

Finally, we estimate Φ_1 . Application of Theorem 5.4 and the triangle inequality yields

$$\|e_c(0)\|^2 \lesssim \|e(0)\|^2 + \|U_{h,d}(0)\|^2 \leq C \eta_I^2. \quad (5.20)$$

Therefore, if we redefine Φ_1 to be

$$\Phi_1 := \left(C \eta_I^2 + C \int_{t^0}^{t^1} \eta_A^2 ds \right)^{1/2} + C \int_{t^0}^{t^1} \eta_B ds,$$

we have

$$\|e_c(t^1)\| \leq \|e_c\|_{L^\infty(t^0, t^1; L^2(\Omega))} \leq \Psi_1, \quad (5.21)$$

where $\Psi_1 := \delta_1 \mathcal{G}_1 \Phi_1$. In the same way, if we redefine

$$\begin{aligned} \Phi_k &:= \left(\Psi_{k-1}^2 + C \int_{t^{k-1}}^{t^k} \eta_A^2 ds \right)^{1/2} + C \int_{t^{k-1}}^{t^k} \eta_B ds, \\ \Psi_k &:= \delta_k \mathcal{G}_k \Phi_k, \end{aligned}$$

we have

$$\|e_c(t^k)\| \leq \|e_c\|_{L^\infty(t^{k-1}, t^k; L^2(\Omega))} \leq \Psi_k. \quad (5.22)$$

Hence, we have shown the following result.

THEOREM 5.7. *The error of the IMEX dG discretization of problem (3.2), given by (4.2), satisfies*

$$\|e\|_{L^\infty(0, T; L^2(\Omega))} \lesssim \Psi_N + \operatorname{ess\,sup}_{0 \leq t \leq T} \left(\sum_{E \in \Gamma(t)} h_E \| [U_h] \|_E^2 \right)^{1/2},$$

providing that the solution to (5.19) exists for all time steps.

Proof. Follows from (5.22), the triangle inequality, and Theorem 5.4. \square

The estimator produced above is suboptimal with respect to the mesh-size as it is only spatially optimal in the $L^2(H^1)$ -norm. It is possible to conduct a continuation argument for the $L^2(H^1)$ -norm rather than the $L^\infty(L^2)$ -norm if one desires a spatially optimal error estimator; this is stated for completeness in the theorem below. However, the resulting δ equation was observed to be more restrictive with regards to how quickly the blow-up time is approached. For this reason, we opt to use the a posteriori error estimator of Theorem 5.7 in the adaptive algorithm introduced in the next section.

THEOREM 5.8. *The error of the IMEX dG discretization of problem (3.2), given by (4.2), satisfies*

$$\left(\|e(T)\|^2 + \int_0^T \varepsilon \|\nabla e_c\|^2 dt \right)^{1/2} \lesssim \sum_{k=1}^N \Psi_k + \operatorname{ess\,sup}_{0 \leq t \leq T} \left(\sum_{E \in \Gamma(t)} h_E \| [U_h] \|_E^2 \right)^{1/2}.$$

Furthermore, close to the blow-up time where $\|e(T)\| = \|e\|_{L^\infty(0, T; L^2(\Omega))}$ we have

$$\left(\|e\|_{L^\infty(0, T; L^2(\Omega))}^2 + \int_0^T \varepsilon \|\nabla e_c\|^2 dt \right)^{1/2} \lesssim \sum_{k=1}^N \Psi_k + \operatorname{ess\,sup}_{0 \leq t \leq T} \left(\sum_{E \in \Gamma(t)} h_E \| [U_h] \|_E^2 \right)^{1/2},$$

where Ψ_k , $k = 1, \dots, N$, is defined recursively with $\Psi_0 = C\eta_I$ and

$$\begin{aligned} \Phi_k &:= \left(\Psi_{k-1}^2 + C \int_{t^{k-1}}^{t^k} \eta_A^2 ds + C \int_{t^{k-1}}^{t^k} \eta_B^2 ds \right)^{1/2}, \\ G_k &:= \exp(\tau_k/2) \exp \left(\int_{t^{k-1}}^{t^k} \sigma_\Omega ds \right), \\ \Psi_k &:= \delta_k \mathcal{G}_k \Phi_k, \end{aligned}$$

provided that $\delta_k > 1$ which is the smallest root of the equation

$$C_{GN}\varepsilon^{-1/2}\tau_k^{1/2}\delta_k G_k \Phi_k - \log(\delta_k) = 0,$$

exists for all time steps.

Proof. The proof is completely analogous to that of Theorem 5.7 and follows from (5.12) by conducting a continuation argument for the $L^\infty(L^2) + L^2(H^1)$ -norm. \square

6. An adaptive algorithm. We shall now proceed by stating our space-time adaptive algorithm for problems with finite time blow-up.

The algorithm is based on Algorithm 2 from Section 2 and the space-time adaptive algorithm for linear evolution problems presented in [10]. It makes use of different terms in the a posteriori bound in Theorem 5.7 to take automatic decisions on space-time refinement and coarsening. The pseudocode describing the adaptive algorithm is given in Algorithm 3.

The term $\eta_{S_1,k}$ drives both local mesh refinement and coarsening. The elements are refined, coarsened or left unchanged depending on two spatial thresholds \mathbf{stol}^+ and \mathbf{stol}^- . Similarly, the term $\eta_{T_2,k}$ is used to drive temporal refinement and coarsening subject to two temporal thresholds \mathbf{ttol}^+ and \mathbf{ttol}^- .

7. Numerical Experiments. We shall investigate numerically the a posteriori bound presented in Theorem 5.7 and the performance of the adaptive algorithm through an implementation based on the `deal.II` finite element library [4]. All the numerical experiments have been performed using the high performance computing facility ALICE at the University of Leicester. The following settings are common to all the numerical experiments presented. We use polynomials of degree five, hence $p = 5$ throughout. This particular choice provides a good compromise between run time and spatial discretization error for the problems considered. Furthermore, it permits us to analyse the asymptotic temporal behaviour of the adaptive algorithm.

Correspondingly, we set $\gamma = 30$ to ensure coercivity of the discrete bilinear form. We also set $\mathbf{ttol}^- = 0.01 * \mathbf{ttol}^+$ and $\mathbf{stol}^- = 10^{-6} * \mathbf{stol}^+$ as, respectively, the temporal and spatial coarsening parameters. The initial mesh ζ^0 is chosen to be a 4×4 uniform quadrilateral mesh and the initial time step length τ_1 is chosen so that the first computed numerical approximation is before the expected blow-up time. The unknown constants in the a posteriori bound are set equal to one as is the constant C_{GN} in (5.19); the above conventions are deemed reasonable for the practical implementation of the a posteriori bound.

7.1. Example 1. We begin by considering a standard reaction-diffusion semi-linear PDE problem whose blow-up behaviour is theoretically well understood. This is given by setting $\Omega = (-4, 4)^2$, $\varepsilon = 1$, $\mathbf{a} = (0, 0)^T$, $f_0 = 0$ and $u_0 = 10e^{-2(x^2+y^2)}$. The initial condition u_0 is chosen to be a Gaussian blob centred on the origin that is chosen large enough so that the solution exhibits blow-up; the blow-up set consists of a single point corresponding to the centre of the Gaussian.

To assess the asymptotic behaviour of the error estimator, we fix a very small spatial threshold so as to render the spatial contribution to both the error and the estimator negligible. We then vary the temporal threshold and record how far the algorithm is able to advance towards the blow-up time. The results are given in Table 7.1.

For the present case (problems without convection), it is known that the solution to (3.2) has the same asymptotic behaviour as the solution to (2.1) with respect to the time variable [27]. Thus, we would expect an effective estimator to yield similar rates

Algorithm 3 Space-time adaptivity

-
- 1: **Input:** $\varepsilon, \mathbf{a}, f_0, u_0, \Omega, \tau_1, \zeta^0, \gamma, \mathbf{ttol}^+, \mathbf{ttol}^-, \mathbf{stol}^+, \mathbf{stol}^-$.
 - 2: Compute U_h^0 .
 - 3: Compute U_h^1 from U_h^0 .
 - 4: **while** $\int_{t^0}^{t^1} \eta_{T_2,1}^2 ds > \mathbf{ttol}^+$ OR $\max_K \eta_{S_1,1}^2|_K > \mathbf{stol}^+$ **do**
 - 5: Modify ζ^0 by refining all elements such that $\eta_{S_1,1}^2|_K > \mathbf{stol}^+$ and coarsening all elements such that $\eta_{S_1,1}^2|_K < \mathbf{stol}^-$.
 - 6: **if** $\int_{t^0}^{t^1} \eta_{T_2,1}^2 ds > \mathbf{ttol}^+$ **then**
 - 7: $\tau_1 \leftarrow \tau_1/2$.
 - 8: **end if**
 - 9: Compute U_h^0 .
 - 10: Compute U_h^1 from U_h^0 .
 - 11: **end while**
 - 12: Compute δ_1 .
 - 13: Multiply $\mathbf{ttol}^+, \mathbf{ttol}^-, \mathbf{stol}^+, \mathbf{stol}^-$ by the factor G_1 .
 - 14: Set $j = 0, \zeta^1 = \zeta^0$.
 - 15: **while** δ_{j+1} exists **do**
 - 16: $j \leftarrow j + 1$.
 - 17: $\tau_{j+1} = \tau_j$.
 - 18: Compute U_h^{j+1} from U_h^j .
 - 19: **if** $\int_{t^j}^{t^{j+1}} \eta_{T_2,j+1}^2 ds > \mathbf{ttol}^+$ **then**
 - 20: $\tau_{j+1} \leftarrow \tau_{j+1}/2$.
 - 21: Compute U_h^{j+1} from U_h^j .
 - 22: **end if**
 - 23: **if** $\int_{t^j}^{t^{j+1}} \eta_{T_2,j+1}^2 ds < \mathbf{ttol}^-$ **then**
 - 24: $\tau_{j+1} \leftarrow 2\tau_{j+1}$.
 - 25: Compute U_h^{j+1} from U_h^j .
 - 26: **end if**
 - 27: Form ζ^{j+1} from ζ^j by refining all elements such that $\eta_{S_1,j+1}^2|_K > \mathbf{stol}^+$ and coarsening all elements such that $\eta_{S_1,j+1}^2|_K < \mathbf{stol}^-$.
 - 28: Compute U_h^{j+1} from U_h^j .
 - 29: Compute δ_{j+1} .
 - 30: Multiply $\mathbf{ttol}^+, \mathbf{ttol}^-, \mathbf{stol}^+, \mathbf{stol}^-$ by the factor G_{j+1} .
 - 31: **end while**
 - 32: **Output:** $j, t^j, \|U_h(t^j)\|_{L^\infty(\Omega)}$.
-

for λ , the difference between the true and numerical blow-up time, to those seen in Section 2. Although the true blow-up time for this problem is not known, we observe from Table 7.1 that

$$\|U_h\|_{L^\infty(0,T;L^\infty(\Omega))} \propto N^{1/2}.$$

From [27], we know the relationship between the magnitude of the exact solution in the $L^\infty(L^\infty)$ -norm and the distance from the blow-up time. Thus, under the assumption

Table 7.1: Example 1 Results

\mathbf{ttol}^+	Time Steps	Estimator	Final Time	$\ U_h(T)\ _{L^\infty(\Omega)}$
1	3	9.5	0.09375	12.244
0.125	8	24.6	0.12500	14.742
$(0.125)^2$	19	54.0	0.14844	18.556
$(0.125)^3$	42	66.7	0.16406	23.468
$(0.125)^4$	92	218.5	0.17969	32.108
$(0.125)^5$	195	1142.4	0.19043	44.217
$(0.125)^6$	405	1506.0	0.19775	60.493
$(0.125)^7$	832	1754.1	0.20313	83.315
$(0.125)^8$	1698	5554.2	0.20728	117.780
$(0.125)^9$	3443	6020.4	0.21014	165.833
$(0.125)^{10}$	6956	33426.7	0.21228	238.705
$(0.125)^{11}$	14008	36375.0	0.21375	343.078
$(0.125)^{12}$	28151	66012.8	0.21478	496.885
$(0.125)^{13}$	56489	157300.0	0.21549	722.884

that the numerical solution is scaling like the exact solution, we have

$$\lambda(\mathbf{ttol}^+, N) \approx \|u\|_{L^\infty(0,T;L^\infty(\Omega))}^{-1} \approx \|U_h\|_{L^\infty(0,T;L^\infty(\Omega))}^{-1}.$$

Therefore, we conjecture that

$$\lambda(\mathbf{ttol}^+, N) \propto N^{-1/2}.$$

Note that the conjectured convergence rate is slower than the comparable results in Section 2; a possible explanation for this will be given in the concluding remarks.

Next we investigate the *numerical blow-up rate* of $\|U_h(t)\|_{L^\infty(\Omega)}$. In particular, we are interested in checking if the numerical blow-up rate coincides with the theoretical one. For this particular example, it is well known, cf. [38, 39], that close to the blow-up time $\|u(t)\|_{L^\infty(\Omega)}$ behaves as

$$\|u(t)\|_{L^\infty(\Omega)} \sim \frac{1}{T^* - t},$$

where T^* denotes the blow-up time. Let us denote the *numerical blow-up time* by t^* which we compute as follows. For the last numerical experiment (with $\mathbf{ttol}^+ = (0.125)^{13}$), we assume that there exists a constant C_N such that

$$\|U_h(t)\|_{L^\infty(\Omega)} = C_N \frac{1}{t^* - t}, \quad t = t^{N-1}, T.$$

Then t^* is computed by

$$t^* = \frac{T\|U_h(T)\|_{L^\infty(\Omega)} - t^{N-1}\|U_h(t^{N-1})\|_{L^\infty(\Omega)}}{\|U_h(T)\|_{L^\infty(\Omega)} - \|U_h(t^{N-1})\|_{L^\infty(\Omega)}}.$$

For this example, the above relation gives $t^* = 0.217055$.

To compute the numerical blow-up rate, we consider all the time nodes t^k , $k = 0, \dots, N$ with $t^N = 0.21375$ (corresponding to the numerical experiment with $\mathbf{ttol}^+ =$

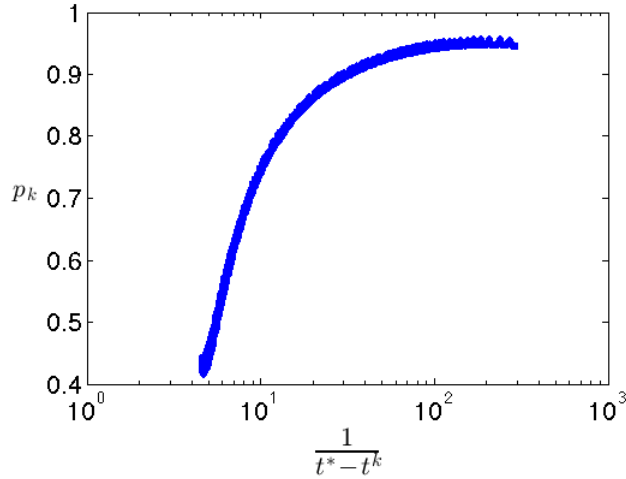


Fig. 7.1: Example 1: Numerical blow-up rate.

$(0.125)^{11}$). Then for every two consecutive times t^{k-1}, t^k we assume that there exists a constant C_k such that

$$\|U_h(t)\|_{L^\infty(\Omega)} = C_k \frac{1}{(t^* - t)^{p_k}}, \quad t = t^{k-1}, t^k,$$

and hence we compute p_k by

$$p_k = \frac{\log(\|U_h(t^k)\|_{L^\infty(\Omega)} / \|U_h(t_{k-1})\|_{L^\infty(\Omega)})}{\log((t^* - t^{k-1}) / (t^* - t^k))}.$$

This produces a sequence $\{p_k\}_{k=1}^N$ of numerical blow-up rates. Since for this example the theoretical blow-up rate is one, for a “correct” asymptotic blow-up rate of the numerical approximation we expect p_k to tend to a number close to one as $k \rightarrow N$. This is indeed the case, as observed in Figure 7.1.

7.2. Example 2. Let $\Omega = (-4, 4)^2$, $\varepsilon = 1$, $\mathbf{a} = (1, 1)^T$, $f_0 = -1$ and $u_0 = 0$. This numerical example is interesting to study as not much is known about blow-up problems with non-symmetric spatial operators. The solution behaves as the solution to a linear convection-diffusion problem for small t . As time progresses, the nonlinear term takes over and the solution begins to exhibit point growth leading to blow-up. As in Example 1, we choose to use a small spatial threshold to render the spatial contribution to both the error and the estimator negligible. We then reduce the temporal threshold and observe how far we can advance towards the blow-up time. The results are given in Table 7.2. From the data, we conclude that

$$\|U_h\|_{L^\infty(0, T; L^\infty(\Omega))} \propto N^{1/2}.$$

Although not much is known about blow-up problems with convection, it is reasonable to assume that because the nonlinear term dominates close to the blow-up time that an analogous relationship between the magnitude of the exact solution in the $L^\infty(L^\infty)$ -norm and distance from the blow-up time exists as in Example 1. Assuming that

Table 7.2: Example 2 Results

ttol^+	Time Steps	Estimator	Final Time	$\ U_h(T)\ _{L^\infty(\Omega)}$
1	4	3.6	0.78125	0.886
0.125	10	3.6	0.97656	1.322
$(0.125)^2$	54	22.0	1.31836	3.269
$(0.125)^3$	119	47.5	1.41602	5.107
$(0.125)^4$	252	132.1	1.48163	8.059
$(0.125)^5$	520	218.4	1.51711	11.819
$(0.125)^6$	1064	664.6	1.54467	18.139
$(0.125)^7$	2158	1466.1	1.56224	27.405
$(0.125)^8$	4354	1421.7	1.57402	41.374
$(0.125)^9$	8792	11423.0	1.58243	64.450
$(0.125)^{10}$	17713	21497.8	1.58770	99.190
$(0.125)^{11}$	35580	21097.1	1.59092	145.785
$(0.125)^{12}$	71352	35862.0	1.59299	211.278

this is indeed the case and following the same reasoning as in Example 1, we again conclude that

$$\lambda(\text{ttol}^+, N) \propto N^{-1/2}.$$

7.3. Example 3. Let $\Omega = (-8, 8)^2$, $\varepsilon = 1$, $\mathbf{a} = (0, 0)^T$, $f_0 = 0$ and the ‘volcano’ type initial condition be given by $u_0 = 10(x^2 + y^2)e^{-0.5(x^2 + y^2)}$. The blow-up set for this example is a circle centred on the origin – this induces layer type phenomena in the solution around the blow-up set as the blow-up time is approached making this example a good test of the spatial capabilities of the adaptive algorithm. Once more, we choose a small spatial threshold so that the spatial contribution to the error and the estimator are negligible. We then reduce the temporal threshold and see how far we can advance towards the blow-up time. The results are given in Table 7.3.

Table 7.3: Example 3 Results

ttol^+	Time Steps	Estimator	Final Time	$\ U_h(T)\ _{L^\infty(\Omega)}$
8	3	15	0.06250	10.371
1	10	63	0.09375	14.194
0.125	36	211	0.11979	21.842
$(0.125)^2$	86	533	0.13412	31.446
$(0.125)^3$	190	971	0.14388	45.122
$(0.125)^4$	404	1358	0.15072	64.907
$(0.125)^5$	880	5853	0.15601	98.048
$(0.125)^6$	1853	10654	0.15942	146.162
$(0.125)^7$	3831	21301	0.16176	219.423
$(0.125)^8$	7851	143989	0.16336	332.849
$(0.125)^9$	16137	287420	0.16442	505.236
$(0.125)^{10}$	32846	331848	0.16512	769.652
$(0.125)^{11}$	66442	626522	0.16558	1175.21

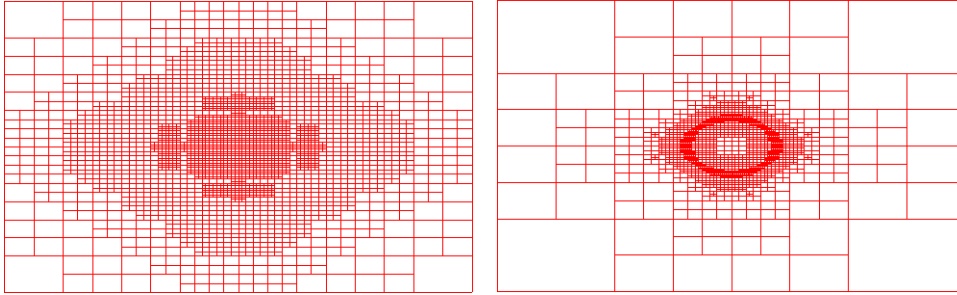


Fig. 7.2: Example 3: Initial (left) and final (right) meshes.

Once again, the data implies that

$$\|U_h\|_{L^\infty(0,T;L^\infty(\Omega))} \propto N^{1/2}.$$

Arguing as in Example 1, we again conclude that

$$\lambda(\mathbf{ttol}^+, N) \propto N^{-1/2}.$$

The numerical solution at $t = 0$ and $t = T$ obtained with the final numerical experiment ($\mathbf{ttol}^+ = (0.125)^{11}$) is shown in Figure 7.3; the corresponding meshes are displayed in Figure 7.2. The initial mesh has a relatively homogenous distribution of elements which is to be expected since the initial condition is relatively smooth. In the final mesh, elements have been added in the vicinity of the blow-up set and removed elsewhere, notably near the origin. The distribution of elements in the final mesh strongly indicates that the adaptive algorithm is adding and removing elements in an efficient manner.

8. Conclusions. We proposed a framework for space-time adaptivity based on rigorous a posteriori bounds for an IMEX dG discretization of a semilinear blow-up problem. The error estimator was applied to a number of test problems and appears to converge towards the blow-up time in all cases. In Section 2, it was observed that the a posteriori error estimator for the related ODE problem with polynomial nonlinearity approaches the blow-up time with a rate of at least one for a basic Euler method. The numerical examples show that, for the PDE blow-up problem, the proposed error estimator appears to be advancing towards the blow-up time at a rate approximately half of that observed for the corresponding ODE error estimator. A possible reason for this behaviour lies in the proof of the a posteriori bound via an energy argument. Nevertheless, it is this very energy argument which delivers a *practical* conditional a posteriori bound in the sense that condition (5.19) can be satisfied within a practically relevant (in terms of computational cost) mesh-parameter regime. It would be interesting to investigate the derivation of conditional a posteriori bounds for fully-discrete schemes for blow-up problems via semigroup techniques, in the spirit of [33], although this currently remains a challenging task.

Acknowledgements. Irene Kyza was supported in part by the European Social Fund (ESF) – European Union (EU) and National Resources of the Greek State within the framework of the Action “Supporting Postdoctoral Researchers” of the Operational Programme “Education and Lifelong Learning (EdLL)”. Stephen Metcalfe

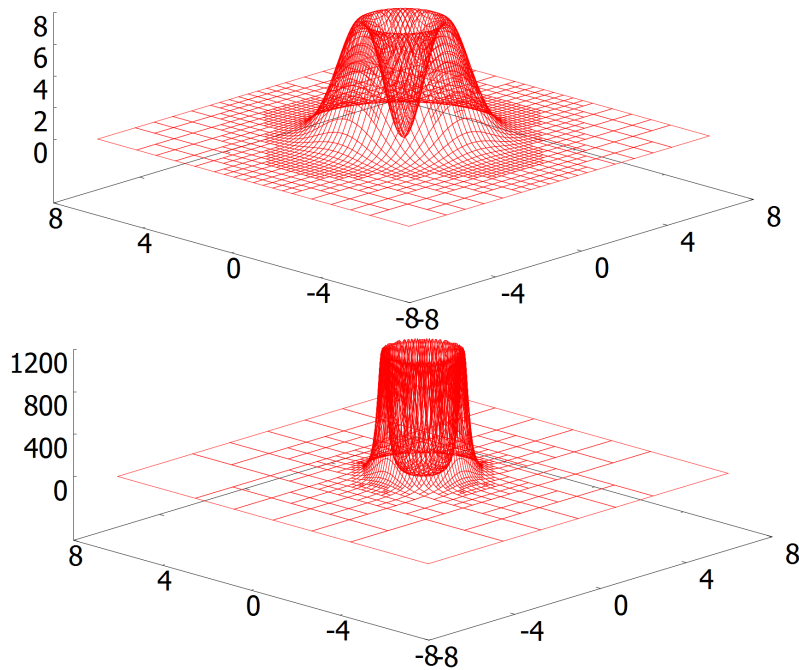


Fig. 7.3: Example 3: Initial (above) and final (below) solution profiles.

gratefully acknowledges the funding of the Engineering and Physical Sciences Research Council (EPSRC). This work originated from a number of visits of the authors to the Archimedes Center for Modelling, Analysis & Computation (ACMAC), which we gratefully acknowledge. We would also like to thank Prof. Theodoros Katsaounis of the University of Crete for suggesting the final numerical example.

REFERENCES

- [1] G. ACOSTA, R. G. DURAN, AND J. D. ROSSI, *An adaptive time step procedure for a parabolic problem with blow-up*, *Computing*, 68 (2002), pp. 343–373.
- [2] GEORGAS D. AKRIVIS, V.A. DOUGALIS, OHANNES A. KARAKASHIAN, AND W.R. MCKINNEY, *Numerical approximation of blow-up of radially symmetric solutions of the nonlinear Schrödinger equation*, *SIAM J. Sci. Comput.*, 25 (2003), pp. 186–212.
- [3] LOUIS A. ASSALÉ, THÉODORE K. BONI, AND DIABATE NABONGO, *Numerical blow-up time for a semilinear parabolic equation with nonlinear boundary conditions*, *J. Appl. Math.*, 2008 (2009).
- [4] W. BANGERTH, R. HARTMANN, AND G. KANSCHAT, *deal.II—a general-purpose object-oriented finite element library*, *ACM Trans. Math. Software*, 33 (2007), pp. Art. 24, 27.
- [5] SÖREN BARTELS, *A posteriori error analysis for time-dependent Ginzburg-Landau type equations*, *Numer. Math.*, 99 (2005), pp. 557–583.
- [6] SÖREN BARTELS AND RÜDIGER MÜLLER, *Quasi-optimal and robust a posteriori error estimates in $L^\infty(L^2)$ for the approximation of Allen-Cahn equations past singularities*, *Math. Comp.*, 80 (2011), pp. 761–780.
- [7] AMAL BERGAM, CHRISTINE BERNARDI, AND ZOUBIDA MGHAZLI, *A posteriori analysis of the finite element discretization of some parabolic equations*, *Math. Comp.*, 74 (2005), pp. 1117–1138.
- [8] MARSHA BERGER AND ROBERT V. KOHN, *A rescaling algorithm for the numerical calculation*

- of blowing-up solutions, *Comm. Pure Appl. Math.*, 41 (1988), pp. 841–863.
- [9] CHRIS J. BUDD, WEIZHANG HUANG, AND ROBERT D. RUSSELL, *Moving mesh methods for problems with blow-up*, *SIAM J. Sci. Comput.*, 17 (1996), pp. 305–327.
- [10] ANDREA CANGIANI, EMMANUIL H. GEORGIOULIS, AND STEPHEN METCALFE, *Adaptive discontinuous Galerkin methods for nonstationary convection-diffusion problems*, *IMA J. Numer. Anal.*, 34 (2014), pp. 1578–1597.
- [11] J.H. CHAUDRY, D. ESTEP, V. GINTING, J.N. SHADID, AND S. TAVENER, *A posteriori error analysis of IMEX multi-step time integration methods for advection-diffusion-reaction equations*, Submitted for publication, (2014).
- [12] JAMES COLEMAN AND CATHERINE SULEM, *Numerical simulation of blow-up solutions of the vector nonlinear Schrödinger equation*, *Phys. Rev. E*, 66 (2002), p. 036701.
- [13] E. CUESTA AND C. MAKRIDAKIS, *A posteriori error estimates and maximal regularity for approximations of fully nonlinear parabolic problems in banach spaces*, *Numer. Math.*, 110 (2008), pp. 257–275.
- [14] JAVIER DE FRUTOS, BOSCO GARCÍA-ARCHILLA, AND JULIA NOVO, *A posteriori error estimates for fully discrete nonlinear parabolic problems*, *Comput. Methods Appl. Mech. Engrg.*, 196 (2007), pp. 3462–3474.
- [15] ARTURO DE PABLO, MAYTE PÉREZ-LLANOS, AND RAÚL FERREIRA, *Numerical blow-up for the p -Laplacian equation with a nonlinear source*, in *Proceedings of the 11th International Conference on Differential Equations (Equadiff05)*, 2005, pp. 363–367.
- [16] A. DEMLOW AND E. H. GEORGIOULIS, *Pointwise a posteriori error control for discontinuous Galerkin methods for elliptic problems*, *SIAM J. Numer. Anal.*, 50 (2012), pp. 2159–2181.
- [17] DANIELE ANTONIO DI PIETRO AND ALEXANDRE ERN, *Mathematical aspects of discontinuous Galerkin methods*, vol. 69 of *Mathématiques & Applications (Berlin) [Mathematics & Applications]*, Springer, Heidelberg, 2012.
- [18] STEFKA DIMOVA, MICHAEL KASCHIEV, MILENA KOLEVA, AND DANIELA VASILEVA, *Numerical analysis of radially nonsymmetric blow-up solutions of a nonlinear parabolic problem*, *J. Comput. Appl. Math.*, 97 (1998), pp. 81–97.
- [19] SEVER SILVESTRU DRAGOMIR, *Some Gronwall type inequalities and applications*, Nova Science Publishers, 2003.
- [20] RAUL FERREIRA, PABLO GROISMAN, AND JULIO D. ROSSI, *Numerical blow-up for a nonlinear problem with a nonlinear boundary condition*, *Math. Models Methods Appl. Sci.*, 12 (2002), pp. 461–483.
- [21] GADI FIBICH AND BOAZ ILAN, *Discretization effects in the nonlinear Schrödinger equation*, *Appl. Numer. Math.*, 44 (2003), pp. 63–75.
- [22] C. FIERRO AND A. VEESER, *On the a posteriori error analysis of equations of prescribed mean curvature*, *Math. Comp.*, 72 (2003), pp. 1611–1634.
- [23] EMMANUIL H. GEORGIOULIS, OMAR LAKKIS, AND JUHA M. VIRTANEN, *A posteriori error control for discontinuous Galerkin methods for parabolic problems*, *SIAM J. Numer. Anal.*, 49 (2011), pp. 427–458.
- [24] EMMANUIL H. GEORGIOULIS AND CHARALAMBOS MAKRIDAKIS, *On a posteriori error control for the Allen-Cahn problem*, *Math. Method. Appl. Sci.*, 37 (2014), pp. 173–179.
- [25] P. GROISMAN, *Totally discrete explicit and semi-implicit euler methods for a blow-up problem in several space dimensions*, *Computing*, 76 (2006), pp. 325–352.
- [26] CHIAKI HIROTA AND KAZUFUMI OZAWA, *Numerical method of estimating the blow-up time and rate of the solution of ordinary differential equations – an application to the blow-up problems of partial differential equations*, *J. Comput. Appl. Math.*, 193 (2006), pp. 614 – 637.
- [27] BEI HU, *Blow-up theories for semilinear parabolic equations.*, vol. 2018 of *Lecture Notes in Mathematics*, Springer, Heidelberg, 2011.
- [28] WEIZHANG HUANG, JINGTANG MA, AND ROBERT D. RUSSELL, *A study of moving mesh PDE methods for numerical simulation of blowup in reaction diffusion equations*, *J. Comput. Phys.*, 227 (2008), pp. 6532–6552.
- [29] B. JANSSEN AND T. P. WIHLER, *Existence Results for the Continuous and Discontinuous Galerkin Time Stepping Methods for Nonlinear Initial Value Problems*, ArXiv e-prints, (2014).
- [30] OHANNES A. KARAKASHIAN AND FREDERIC PASCAL, *A posteriori error estimates for a discontinuous Galerkin approximation of second-order elliptic problems*, *SIAM J. Numer. Anal.*, 41 (2003), pp. 2374–2399 (electronic).
- [31] DANIEL KESSLER, RICARDO H. NOCHETTO, AND ALFRED SCHMIDT, *A posteriori error control for the Allen-Cahn problem: circumventing Gronwall’s inequality*, *ESAIM Math. Model. Numer. Anal.*, 38 (2004), pp. 129–142.

- [32] CHRISTIAN KLEIN, BENSON MUIITE, AND KRISTELLE ROIDOT, *Numerical study of blowup in the Davey-Stewartson system*, arXiv preprint arXiv:1112.4043, (2011).
- [33] I. KYZA AND C. MAKRIDAKIS, *Analysis for time discrete approximations of blow-up solutions of semilinear parabolic equations*, SIAM J. Numer. Anal., 49 (2011), pp. 405–426.
- [34] OMAR LAKKIS AND CHARALAMBOS MAKRIDAKIS, *Elliptic reconstruction and a posteriori error estimates for fully discrete linear parabolic problems*, Math. Comp., 75 (2006), pp. 1627–1658.
- [35] O. LAKKIS AND R. H. NOCHETTO, *A posteriori error analysis for the mean curvature flow of graphs*, SIAM J. Numer. Anal., 42 (2005), pp. 1875–1898.
- [36] CHARALAMBOS MAKRIDAKIS AND RICARDO H. NOCHETTO, *Elliptic reconstruction and a posteriori error estimates for parabolic problems*, SIAM J. Numer. Anal., 41 (2003), pp. 1585–1594.
- [37] C. MAKRIDAKIS AND R. H. NOCHETTO, *A posteriori error analysis for higher order dissipative methods for evolution problems*, Numer. Math., 104 (2006), pp. 489–514.
- [38] FRANK MERLE AND HATEM ZAAG, *Optimal estimates for blowup rate and behavior for nonlinear heat equations*, Communications on pure and applied mathematics, 51 (1998), pp. 139–196.
- [39] ———, *A Liouville theorem for vector-valued nonlinear heat equations and applications*, Math. Ann., 316 (2000), pp. 103–137.
- [40] F. K. N’GOHISSE AND THÉODORE K. BONI, *Numerical blow-up for a nonlinear heat equation*, Acta Math. Sin. (Engl. Ser.), 27 (2011), pp. 845–862.
- [41] V.T. NGUYEN AND H. ZAAG, *Blow-up results for a strongly perturbed semilinear heat equation: Theoretical analysis and numerical method*, (2014).
- [42] MICHAEL PLEXOUSAKIS, *An adaptive nonconforming finite element method for the nonlinear Schrödinger equation*, PhD thesis, University of Tennessee, 1996.
- [43] DOMINIK SCHÖTZAU AND LIANG ZHU, *A robust a-posteriori error estimator for discontinuous Galerkin methods for convection-diffusion equations*, Appl. Numer. Math., 59 (2009), pp. 2236–2255.
- [44] A.M. STUART AND M.S. FLOATER, *On the computation of blow-up*, Euro. J. Appl. Math., 1 (1990), pp. 47–71.
- [45] Y. TOURIGNY AND J.M. SANZ-SERNA, *The numerical study of blowup with application to a nonlinear Schrödinger equation*, J. Comput. Phys., 102 (1992), pp. 407–416.
- [46] R. VERFÜRTH, *A posteriori error estimates for nonlinear problems: $L^r(0, t; L^p(\Omega))$ -error estimates for finite element discretizations of parabolic equations*, Math. Comp., 67 (1998), pp. 1335–1360.
- [47] ———, *A posteriori error estimates for nonlinear problems: $L^r(0, t; W^{1,p}(\Omega))$ -error estimates for finite element discretizations of parabolic equations*, Numer. Methods Partial Differential Equations, 14 (1998), pp. 487–518.
- [48] ———, *A posteriori error estimates for non-linear parabolic equations*, Preprint, Ruhr-Universität Bochum, Fakultät für Mathematik, Bochum, Germany, (2004).